ANALYZING THE CHARACTERISTIC MAP OF TRIANGULAR SUBDIVISION SCHEMES

GEORG UMLAUF*

Abstract. Tools for the analysis of generalized triangular box spline subdivision schemes are developed. For the first time the full analysis of Loop's algorithm can be carried out with these tools.

Key words. Subdivision, triangular schemes, Loop's algorithm, box splines.

AMS subject classifications. 65D17, 65D07, 68U07

Abbreviated title. Characteristic Map of Triangular Subdivision Schemes

1. Introduction. In the last two decades many subdivision schemes for different purposes were devised, see e.g. [2, 1, 6, 11, 3, 4, 7]. All these algorithms generate from an initial control net a sequence of nets which converges to a limiting surface. Although sufficient conditions for the convergence to a smooth limiting surface were given in [12] and [9], their rigorous application has been carried out only for some of the above mentioned schemes by Peters and Reif [8, 7].

In this paper we will investigate the smoothness of the limiting surfaces obtained by subdivision algorithms for triangular nets. According to the sufficient conditions of [12] and [9], we have to analyze the spectral properties of the subdivision matrix associated with the algorithm and the so-called characteristic map. Symmetry properties of the algorithms help to simplify this analysis significantly.

Subsequently the analysis is carried out for Loop's algorithm [6]. The spectral properties of the subdivision matrix imply some characteristics of the algorithm as already observed by Loop [6]. To prove regularity and injectivity of the characteristic map we use its Bézier representation as in [13] and [8]. This leads to a rigorous proof of tangent continuity of the limiting surface of Loop's algorithm.

2. Generalized subdivision. We presume that all subdivision algorithms considered here are *stationary*, *local*, and *linear* schemes for tri- or quadrilateral nets. Such an algorithm generates starting from an initial arbitrary tri- or quadrilateral net $\mathbf{C}_0$ a sequence of ever finer nets $\{\mathbf{C}_m\}_{m=0}^{\infty}$. Thereby only finite, affine combinations, represented by so called *masks*, are used to compute the points of the net $\mathbf{C}_m$ from $\mathbf{C}_{m-1}, m \geq 1$. This makes up for the locality and linearity of these schemes. Since we use the same affine combinations in every step m of the iteration, the subdivision algorithm is said to be stationary.

The sequence of nets $\{\mathbf{C}_m\}_{m=0}^{\infty}$ generated by such an algorithm will eventually converge to a limiting surface $\mathbf{s}$ consisting of infinitely many tri- or quadrilateral patches.

An example for Loop's algorithm is shown in Figure 2.1. The upper left net is the initial net $\mathbf{C}_0$. The other nets $\mathbf{C}_1, \ldots, \mathbf{C}_4$ are the result of the first four iterations of Loop's algorithm starting from $\mathbf{C}_0$.

Suppose that on the regular parts of a net, i.e. parts of the net that contain only *ordinary vertices* of valence 6 or 4 for tri- or quadrilateral nets respectively, standard

*Fakultät für Informatik, Universität Karlsruhe, D-76128 Karlsruhe, Germany, umlauf@ira.uka.de. Supported by DFG grant # PR 565/1-1.

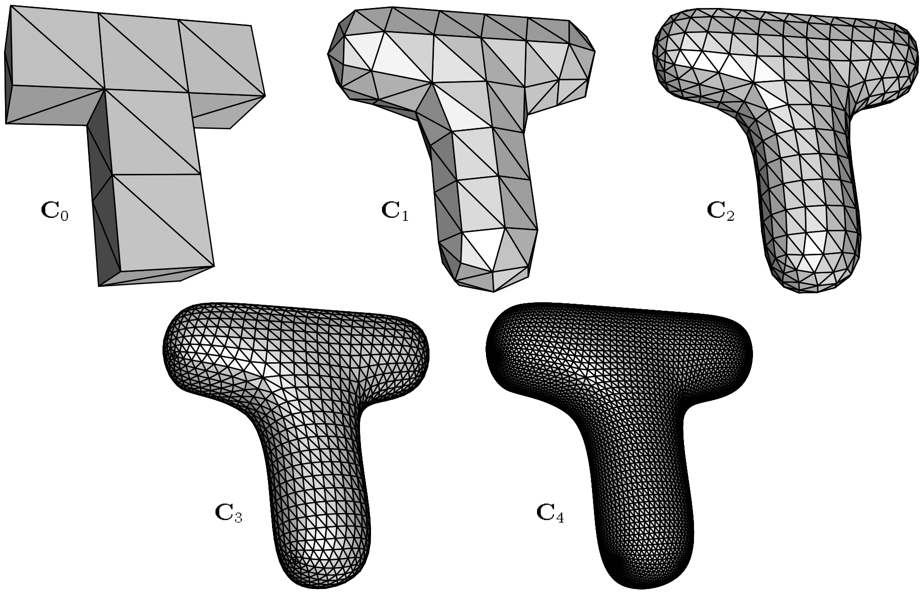

FIG. 2.1. *The initial triangular net* $\mathbf{C}_0$ *(top left) and the nets* $\mathbf{C}_1, \ldots, \mathbf{C}_4$ *of the first four iteration steps of Loop's algorithm.*

subdivision rules for symmetric box splines apply. Examples for such standard subdivision rules are the subdivision rules for tensorproduct splines [5] or for quartic box splines over the three-directional grid. On this condition the regular parts of a net determine C^k-surfaces.

Near vertices of valence $\neq 6$ ($\neq 4$) for tri- (quadri-)lateral nets, the so-called *extraordinary vertices*, special subdivision rules are used, which do not change the number of extraordinary vertices in two consecutive nets $\mathbf{C}_{m-1}$ and $\mathbf{C}_m$, $m \geq 2$. Since the subdivision masks of stationary, local schemes have fixed finite size, we can restrict the analysis to nets $\mathbf{C}_0$ with a single extraordinary vertex surrounded by r rings of ordinary vertices. An example is illustrated in Figure 2.2 for $r = 3$.

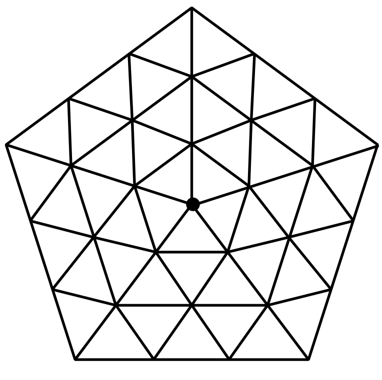

FIG. 2.2. *An initial net* $\mathbf{C}_0$ *with an extraordinary vertex of valence 5 (marked by* $\bullet$*) surrounded by* $r = 3$ *rings of ordinary vertices.*

The particular choice of r depends on the subdivision algorithm. It must be such that the regular parts of $\mathbf{C}_0$ define at least one complete surface ring. Loop's algorithm requires for example $r = 3$.

If we denote by $\mathbf{s}_m$ the surface that corresponds to the regular parts of $\mathbf{C}_m$, then the limiting surface is given by $\mathbf{s} = \cup \mathbf{s}_m$. Obviously $\mathbf{s}_{m-1}$ is part of $\mathbf{s}_m$ for $m \geq 1$. So taking $\mathbf{s}_{m-1}$ away from $\mathbf{s}_m$ we obtain a surface ring $\mathbf{r}_m$ which is added to $\mathbf{s}_{m-1}$ in the mth iteration step. This yields $\mathbf{s} = \mathbf{s}_0 \cup \bigcup_{m \geq 1} \mathbf{r}_m$.

At an extraordinary vertex of valence n the surface rings $\mathbf{r}_m$ can be parametrized over a common domain $\Omega \times \mathbb{Z}_n$ in terms of a subnet $\mathbf{D}_m \subset \mathbf{C}_m$ and certain functions N^k. If $\mathbf{d}_m^0, \ldots, \mathbf{d}_m^K$ denote the vertices of $\mathbf{D}_m$, we have

$$\mathbf{r}_m : \Omega \times \mathbb{Z}_n \to \mathbb{R}^3$$
$$(u, v, j) \mapsto \mathbf{r}_m^j(u, v) = \sum_{k=0}^{K} \mathbf{d}_m^k \, N^k(u, v, j) =: N(u, v, j) \, \mathbf{d}_m,$$

where Ω is either

$$\Omega^{\triangle} = \{(u, v) | u, v \geq 0 \text{ and } 1 \leq u + v \leq 2\}$$

in case of trilateral nets or

$$\Omega^{\square} = \{(u, v) | u, v \geq 0 \text{ and } 1 \leq \max\{u, v\} \leq 2\}$$

in case of quadrilateral nets, see Figure 2.3.

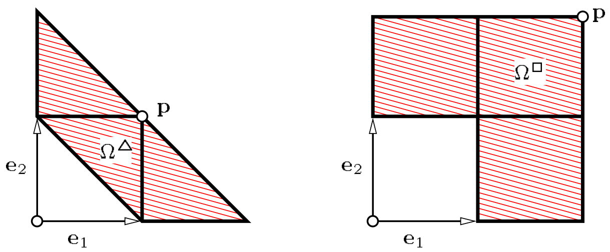

FIG. 2.3. *The domains* $\Omega^{\triangle}$ *(left) and* $\Omega^{\square}$ *(right).*

Note that all nets $\mathbf{D}_m$ have equally many vertices. Hence the stationary, local, and linear subdivision algorithm can be described by a square *subdivision matrix* A, i.e.

$$\mathbf{d}_m = A \mathbf{d}_{m-1}.$$

3. The subdivision matrix and the characteristic map. Let $\lambda_0, \ldots, \lambda_K$ be the eigenvalues of A listed with all their algebraic multiplicities and ordered by their modulus

$$|\lambda_0| \geq |\lambda_1| \geq \ldots \geq |\lambda_K|$$

and denote by $\mathbf{v}_0, \ldots, \mathbf{v}_K$ the corresponding generalized eigenvectors. If $|\lambda_0| > |\lambda_1| = |\lambda_2| > |\lambda_3|$, the two dimensional surface that is defined by the net $[\mathbf{v}_1, \mathbf{v}_2]$

$$\mathbf{x}(u, v, j) := N(u, v, j) \, [\mathbf{v}_1, \mathbf{v}_2] : \Omega \times \mathbb{Z}_n \to \mathbb{R}^2$$

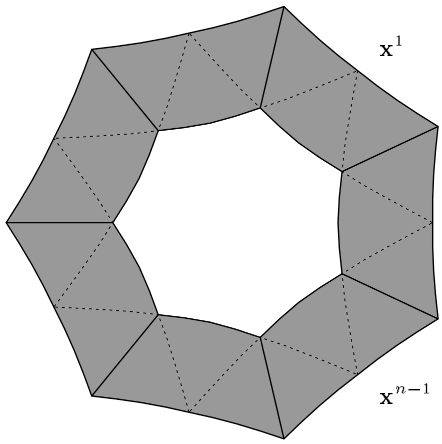

FIG. 3.1. *The characteristic map of Loop's algorithm for $n = 7$.*

is called the *characteristic map* of the subdivision scheme [12]. Note that $\mathbf{x}$ can be regarded as consisting of n *segments* $\mathbf{x}^j(u,v) := \mathbf{x}(u,v,j)$. An example for the characteristic map of Loop's algorithm is shown in Figure 3.1.

The crucial theorem for the analysis of subdivision algorithms can now be stated in terms of the *subdominant eigenvalue* $\lambda := \lambda_2 = \lambda_3$ and $\mathbf{x}$:

THEOREM 3.1. *Let λ be a real eigenvalue with geometric multiplicity 2. If the characteristic map $\mathbf{x}$ is regular and injective and*

$$\lambda_0 = 1 > |\lambda| > |\lambda_3|,$$

then the limiting surface is a C^1-manifold for almost all initial control nets $\mathbf{C}_0$.

Proofs of this theorem can be found in [12] or in a more general setting in [9].

In the sequel we apply Theorem 3.1 to subdivision schemes with two additional properties.

1. A subdivision algorithm is said to be *symmetric*, if it is invariant under shifts and reflections of the labelling of $\mathbf{d}_m$. This means if permutation matrices S and R characterized by

$$N(u,v,j+1)\mathbf{d}_m = N(u,v,j)S\mathbf{d}_m \quad \text{and}$$
$$N(v,u,-j)\mathbf{d}_m = N(u,v,j)R\mathbf{d}_m$$

exist, then A commutes with S and R:

$$AS = SA \quad \text{and} \quad AR = RA.$$

Note that S and R exist especially for subdivision algorithms based on box splines with regular hexagonal or square support.

2. A subdivision algorithm is said to have a *normalized* characteristic map, if $\mathbf{x}^0(\mathbf{p}) = (p,0)$ with $p > 0$ and $\mathbf{p} = \mathbf{e}_1 + \mathbf{e}_2$ or $\mathbf{p} = 2\mathbf{e}_1 + 2\mathbf{e}_2$ in case of tri- or quadrilateral nets, respectively, see Figure 2.3.

The first property implies that the subdivision matrix A has a block-circulant structure with square blocks $A_j, j = 0, \ldots, n-1$. Thus A is unitary similar to a block-diagonal matrix $\widehat{A}$. The diagonal blocks of $\widehat{A}$ result from A_j by the discrete Fourier transform:

$$\widehat{A}_j = \sum_{k=0}^{n-1} \omega_n^{-jk} A_k \qquad \text{for } j = 0, \ldots, n-1,$$

where $\omega_n = \exp(2\pi i/n)$ denotes an n-th root of unity. This means, if $\widehat{\mathbf{v}}$ is an eigenvector of some block $\widehat{A}_j$ corresponding to the eigenvalue μ, then μ is also an eigenvalue of A with eigenvector

$$\mathbf{v} = [\omega_n^0 \widehat{\mathbf{v}}, \omega_n^j \widehat{\mathbf{v}}, \ldots, \omega_n^{j(n-1)} \widehat{\mathbf{v}}]. \tag{3.1}$$

If * denotes the complex-conjugate, the blocks of $\widehat{A}$ satisfy $\widehat{A}_j = \widehat{A}^*_{n-j}$ for $j = 1, \ldots, \lfloor n/2 \rfloor$. Hence there are always two linear independent, real eigenvectors $\mathbf{v}_1 = \Re(\mathbf{v})$ and $\mathbf{v}_2 = \Im(\mathbf{v})$ corresponding to the real subdominant eigenvalue λ. From this a first necessary condition for the subdominant eigenvalue can easily be deduced [8]:

LEMMA 3.2. *The characteristic map of a symmetric subdivision scheme in not injective, if the subdominant eigenvalue is from a block $\widehat{A}_j$ for $j \neq 1, n-1$.*

Equation (3.1) shows also that normalization of an injective characteristic map can always be achieved by an appropriate scaling of $\widehat{\mathbf{v}}$.

4. Sufficient conditions for regularity and injectivity. Throughout this chapter we will assume that the subdominant eigenvalue λ is a real eigenvalue from the blocks $\widehat{A}_1$ and $\widehat{A}_{n-1}$.

The two properties of the last chapter imply that the characteristic map $\mathbf{x}$ is symmetric under rotations and reflections for subdivision schemes for tri- or quadrilateral nets ([8]). They allow us to restrict the analysis of the characteristic map to its single segment $\mathbf{x}^0$:

THEOREM 4.1. *Let $\mathbf{x}^0 = [x, y]$ and denote by $\mathbf{x}^0_v := [x_v, y_v]$ the partial derivatives of $\mathbf{x}^0$ with respect to v. If the normalized characteristic map $\mathbf{x}$ of a symmetric subdivision scheme for quadrilateral nets satisfies*

$$\mathbf{x}^0_v(u, v) > \mathbf{0} \qquad \text{for all } (u, v) \in \Omega^\square$$

componentwise, then the characteristic map is regular and injective.

For a proof of this theorem see [8]. The proof also applies to any map $\mathbf{z} : \Omega^\square \times \mathbb{Z}_n \to \mathbb{R}^2$ that shares the above symmetry properties of the map $\mathbf{x}$.

Theorem 4.1 can be transfered to triangular nets by the observation that any triangular net as in Figure 2.2 can be viewed as a quadrilateral net with diagonal edges. This is shown in Figure 4.1 for the domains $\Omega^\triangle$ and $\Omega^\square$.

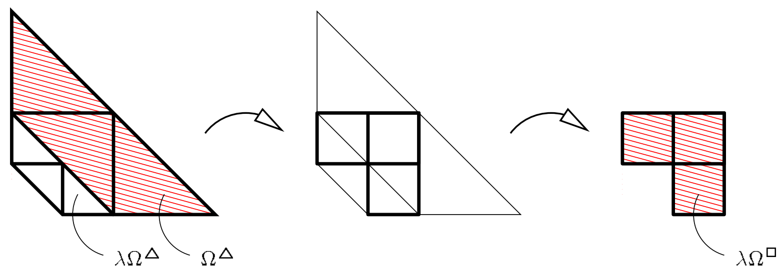

FIG. 4.1. *Converting a triangular to a quadrilateral net.*

In case of triangular nets the domain of the characteristic map $\mathbf{y}$ consists of n plane copies of $\Omega^{\triangle}$. Further we have $\lambda\Omega^{\square} \subset \lambda\Omega^{\triangle} \cup \Omega^{\triangle}$, as illustrated in Figure 4.1. Define the map $\mathbf{z}$ as

$$\mathbf{z} : \lambda\Omega^{\square} \times \mathbb{Z}_n \to \mathbb{R}^2$$
$$(u, v, j) \mapsto \begin{cases} \mathbf{y}^j(u,v) & \text{if } (u,v) \in \Omega^{\triangle} \\ \lambda\mathbf{y}^j(u,v) & \text{if } (u,v) \in \lambda\Omega^{\triangle} \end{cases} .$$

Thus $\mathbf{z}$ is "covered" by $\mathbf{y}$ and $\lambda\mathbf{y}$ and adopts its symmetry properties. Hence Theorem 4.1 is valid for the map $\mathbf{z}$ and can be applied to subdivision schemes for triangular nets, if $\mathbf{x}$ is replaced by $\mathbf{y}$ and $\Omega^{\square}$ by $\Omega^{\triangle}$:

THEOREM 4.2. *If for the normalized characteristic map* $\mathbf{y}$ *of a symmetric subdivision scheme for triangular nets the segment* $\mathbf{y}^0$ *satisfies*

$$\mathbf{y}^0_v(u,v) > \mathbf{0} \qquad \text{for all } (u,v) \in \Omega^{\triangle}$$

componentwise, then the map $\mathbf{z}$ *is regular and injective.*

In practice we will use the Bézier representation of $\mathbf{y}^0$ to apply Theorem 4.2. Hence the proof of the positivity of $\mathbf{y}^0_v$ for all $(u,v) \in \Omega^{\triangle}$ reduces to the proof of the positivity of its Bézier points.

COROLLARY 4.3. *If all Bézier points of* $\mathbf{y}^0_v$ *are positive, then the normalized characteristic map* $\mathbf{y}$ *of a symmetric subdivision scheme for triangular nets is regular and injective.*

5. Loop's algorithm. Loop's algorithm is a generalization of the subdivision scheme for quartic box-splines over a regular triangular grid. The masks are given in Figure 5.1, where the parameter α can be chosen arbitrarily from the interval

$$\big(-\cos(2\pi/n)/4, (3+\cos(2\pi/n))/4\big) . \tag{5.1}$$

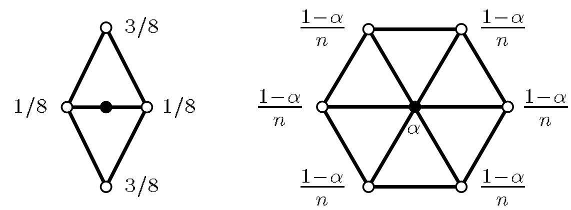

FIG. 5.1. *The masks of Loop's algorithm.*

The limiting surface generated by this algorithm is a piecewise quartic C^2-surface except at its extraordinary points. Here the surface is conjectured to be tangent continuous, see [6].

Obviously, Loop's algorithm is a symmetric scheme. The form of its subdivision matrix A depends on the labelling of the vertices in the control net $\mathbf{D}_m$. If we label them segment after segment counterclockwise as in Figure 5.2 the subdivision matrix A has a block-circulant structure:

$$A = \begin{bmatrix} A_0 & A_1 & \cdots & A_{n-1} \\ A_{n-1} & A_0 & \cdots & A_{n-2} \\ \vdots & & \ddots & \vdots \\ A_1 & \cdots & A_{n-1} & A_0 \end{bmatrix} \in \mathbb{R}^{7n \times 7n}.$$

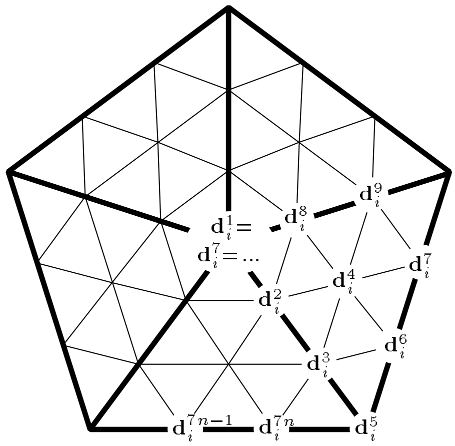

FIG. 5.2. *The labelling of the vertices of the control net* $\mathbf{D}_m$ *for* $n = 5$.

Now we can use the discrete Fourier transform as in Chapter 3 to yield a unitary similar block-diagonal matrix $\widehat{A}$ with blocks

$$\widehat{A}_0 = \left[\begin{array}{c|c|cc|ccc} \alpha & 1-\alpha & & & & & \\ \hline 3/8 & 5/8 & & & & & \\ \hline 1/16 & 3/4 & 1/16 & 1/8 & & & \\ 1/8 & 3/4 & 0 & 1/8 & & & \\ \hline 0 & 3/8 & 3/8 & 1/4 & 0 & 0 & 0 \\ 0 & 1/2 & 1/8 & 3/8 & 0 & 0 & 0 \\ 0 & 1/2 & 1/8 & 3/8 & 0 & 0 & 0 \end{array}\right] \quad \text{and}$$

$$\widehat{A}_j = \left[\begin{array}{c|c|cc|ccc} 0 & & & & & & \\ \hline 0 & 3/8 + c_n^j/4 & & & & & \\ \hline 0 & 5/8 + c_n^j/8 & 1/16 & 1/16 + \omega_n^j/16 & & & \\ 0 & 3/8 + 3\omega_n^{-j}/8 & 0 & 1/8 & & & \\ \hline 0 & 3/8 & 3/8 & 1/8 + \omega_n^j/8 & 0 & 0 & 0 \\ 0 & 3/8 + \omega_n^{-j}/8 & 1/8 & 3/8 & 0 & 0 & 0 \\ 0 & 1/8 + 3\omega_n^{-j}/8 & \omega_n^{-j}/8 & 3/8 & 0 & 0 & 0 \end{array}\right]$$

for $j = 1, \ldots, n-1$ and $c_n^j + is_n^j = \omega_n^j$. From this we get the eigenvalues of the subdivision matrix A as follows:

- 1,
- $\mu_\alpha := \alpha - 3/8$,
- $\mu_j := 3/8 + c_n^j/4$ for $j = 1, \ldots, n-1$,
- $1/8$ and $1/16$ each n-fold and
- 0 which occurs $(4n-1)$-fold.

Note that $\mu_j = \mu_{n-j}$ for $j = 1, \ldots, \lfloor n/2 \rfloor$ and $\mu_1 > \mu_j$ for $j = 2, \ldots, \lfloor n/2 \rfloor$. Furthermore $\widehat{A}_1 = \widehat{A}_{n-1}^*$, so that μ_1 has geometric multiplicity 2. Therefore μ_1 is the double subdominant eigenvalue λ of A, if $|\mu_\alpha| < \mu_1$. This last inequality yields the interval (5.1) for α given by [6].

This verifies the conditions of Theorem 3.1 for the subdominant eigenvalue of the subdivision matrix. What remains is the analysis of the characteristic map.

REMARK 5.1. *The spectral analysis of A can also be used to modify the subdivision* *algorithm so as to generate smoother limiting surfaces [10].*

6. The characteristic map of Loop's algorithm. According to Corollary 4.3 we only need to show positivity of the Bézier points of $\mathbf{y}_v^0$ to proof regularity and injectivity of the characteristic map $\mathbf{y}$ of Loop's algorithm.

Some calculations using a computer algebra system yield the Bézier points of $\mathbf{y}_v^0$ as given in Figure 6.1. Except for positive constants the denominators are given by

$$D_n^1 = 5 + 4c_n^1,$$
$$D_n^2 = 54 + 36c_n^1,$$
$$D_n^3 = 19 + 22c_n^1 + 4c_n^2.$$

Obviously D_n^1, D_n^2, D_n^3 are positive for arbitrary $n \geq 3$ since $c_n^1 \geq -1/2$.

The numerators in Figure 6.1 are of the form

$$E_n^c = a_0 + a_1 c_n^1 + a_2 c_n^2 + a_3 c_n^3, \qquad a_0, a_1, a_2, a_3 \in \mathbb{Z}, \qquad \text{or}$$
$$E_n^s = b_1 s_n^1 + b_2 s_n^2 + b_3 s_n^3, \qquad b_1, b_2, b_3 \in \mathbb{Z}.$$

Since $a_0, a_1 > 0$, the numerators E_n^c are positive if

$$a_0 > a_1/2 + |a_2| + |a_3|.$$

This last condition is fulfilled by all E_n^c. The positivity of the other numerators E_n^s for $n \geq 3$ can be shown in a similar fashion. This completes the proof for

LEMMA 6.1. *Loop's algorithm generates C^1-manifolds for almost all initial triangular nets $\mathbf{C}_0$.*

REMARK 6.2. *This proof applies also to the subdivision schemes proposed in [10]. Thus these schemes generate curvature continuous surfaces with flat spots at the extraordinary points for almost all initial triangular nets $\mathbf{C}_0$.*

REFERENCES

[1] E. CATMULL AND J. CLARK, *Recursive generated b-spline surfaces on arbitrary topological meshes*, Computer Aided-Design, 10 (1978), pp. 350–355.

[2] D. DOO AND M. SABIN, *Behaviour of recursive division surfaces near extraordinary points*, Computer Aided-Design, 10 (1978), pp. 356–360.

[3] N. DYN, J. GREGORY, AND D. LEVIN, *A butterfly subdivision scheme for surface interpolation with tension control*, ACM Transactions on Graphics, 9 (1990), pp. 160–169.

[4] L. KOBBELT, *Iterative Erzeugung glatter Interpolanten*, PhD thesis, IBDS, Universität Karlsruhe, 1995. Verlag Shaker, Aachen.

[5] J. LANE AND R. RIESENFELD, *A Theoretical Development for the Computer Generation and Display of Piecewise Polynomial Surfaces*, IEEE Transactions on Pattern Analysis and Machine Intelligence, 2 (1980), pp. 35–46.

[6] C. LOOP, *Smooth Subdivision Surfaces Based on Triangles*, master's thesis, Department of Mathematics, University of Utah, Aug. 1987.

[7] J. PETERS AND U. REIF, *The simplest subdivision scheme for smoothing polyhedra*, ACM Transactions on Graphics, 16 (1997), pp. 420–431.

[8] ———, *Analysis of algorithms generalizing b-spline subdivision*, SIAM Journal on Numerical Analysis, 35 (1998), pp. 728–748.

[9] H. PRAUTZSCH, *Analysis of C^k-subdivision surfaces at extraordinary points*, preprint 98/4, Fakultät für Informatik, Universität Karlsruhe, 1998. `http://i33www.ira.uka.de`.

[10] H. PRAUTZSCH AND G. UMLAUF, *Improved triangular subdivision schemes*, in Computer Graphics International 1998, F.-E. Wolter and N. Patrikalakis, eds., Hannover, 22.-26. Juni 1998, IEEE Computer Society, pp. 626–632.

[11] R. QU, *Recursive subdivision algorithms for curve and surface design*, PhD thesis, Department of Mathematics and Statistics, Burnel University, Uxbridge, Middlesex, England, Aug. 1990.

$$\begin{bmatrix}\frac{80+82c_n^1-2c_n^2-4c_n^3}{9D_n^3}\\ \frac{78s_n^1+6s_n^2-4s_n^3}{9D_n^3}\end{bmatrix}$$

$$\begin{bmatrix}\frac{80+88c_n^1+4c_n^2-4c_n^3}{9D_n^3}\\ \frac{72s_n^1+12s_n^2-4s_n^3}{9D_n^3}\end{bmatrix}\begin{bmatrix}\frac{84+80c_n^1-2c_n^2}{9D_n^3}\\ \frac{72s_n^1+12s_n^2-2s_n^3}{9D_n^3}\end{bmatrix}$$

$$\begin{bmatrix}\frac{40+35c_n^1-7c_n^2-2c_n^3}{18D_n^1}\\ \frac{45s_n^1-3s_n^2-2s_n^3}{18D_n^1}\end{bmatrix}\begin{bmatrix}\frac{55+56c_n^1+2c_n^2-2c_n^3}{6D_n^3}\\ \frac{66s_n^1+18s_n^2-s_n^3}{9D_n^3}\end{bmatrix}\begin{bmatrix}\frac{171+148c_n^1-6c_n^2-4c_n^3}{18D_n^3}\\ \frac{22s_n^1+6s_n^2}{3D_n^3}\end{bmatrix}$$

$$\begin{bmatrix}\frac{40+41c_n^1-c_n^2-2c_n^3}{18D_n^1}\\ \frac{39s_n^1+3s_n^2-2s_n^3}{18D_n^1}\end{bmatrix}\begin{bmatrix}\frac{44+33c_n^1-5c_n^2}{18D_n^1}\\ \frac{13s_n^1+s_n^2}{6D_n^1}\end{bmatrix}\begin{bmatrix}\frac{165+152c_n^1-6c_n^2-8c_n^3}{18D_n^3}\\ \frac{60s_n^1+24s_n^2+2s_n^3}{9D_n^3}\end{bmatrix}\begin{bmatrix}\frac{57+44c_n^1-6c_n^2-2c_n^3}{6D_n^3}\\ \frac{60s_n^1+24s_n^2+2s_n^3}{9D_n^3}\end{bmatrix}$$

$$\begin{bmatrix}\frac{44+39c_n^1+c_n^2}{18D_n^1}\\ \frac{11s_n^1+3s_n^2}{6D_n^1}\end{bmatrix}\begin{bmatrix}\frac{46+27c_n^1-7c_n^2}{18D_n^1}\\ \frac{11s_n^1+3s_n^2}{6D_n^1}\end{bmatrix}\begin{bmatrix}\frac{165+136c_n^1-18c_n^2-10c_n^3}{18D_n^3}\\ \frac{20s_n^1+4s_n^2}{D_n^2}\end{bmatrix}\begin{bmatrix}\frac{171+116c_n^1-30c_n^2-8c_n^3}{18D_n^3}\\ \frac{20s_n^1+4s_n^2}{D_n^2}\end{bmatrix}$$

$$\begin{bmatrix}\frac{44+39c_n^1+c_n^2}{18D_n^1}\\ \frac{5s_n^1+s_n^2}{18}\end{bmatrix}\begin{bmatrix}\frac{47+21c_n^1-11c_n^2}{18D_n^1}\\ \frac{9s_n^1+5s_n^2}{6D_n^1}\end{bmatrix}\begin{bmatrix}\frac{81+58c_n^1-18c_n^2-7c_n^3}{9D_n^3}\\ \frac{48s_n^1+36s_n^2+7s_n^3}{9D_n^3}\end{bmatrix}\begin{bmatrix}\frac{28+16c_n^1-8c_n^2-2c_n^3}{3D_n^3}\\ \frac{16s_n^1+12s_n^2+2s_n^3}{3D_n^3}\end{bmatrix}$$

$$\begin{bmatrix}\frac{41+19c_n^1-17c_n^2-4c_n^3}{18D_n^1}\\ \frac{21s_n^1+21s_n^2+4s_n^3}{18D_n^1}\end{bmatrix}\begin{bmatrix}\frac{45+11c_n^1-21c_n^2-2c_n^3}{18D_n^1}\\ \frac{21s_n^1+21s_n^2+2s_n^3}{18D_n^1}\end{bmatrix}\begin{bmatrix}\frac{78+46c_n^1-30c_n^2-10c_n^3}{9D_n^3}\\ \frac{42s_n^1+42s_n^2+10s_n^3}{9D_n^3}\end{bmatrix}\begin{bmatrix}\frac{82+38c_n^1-34c_n^2-8c_n^3}{9D_n^3}\\ \frac{42s_n^1+42s_n^2+8s_n^3}{9D_n^3}\end{bmatrix}$$

FIG. 6.1. *The Bézier points of* $\mathbf{y}_v^0$.

[12] U. Reif, *A unified approach to subdivision algorithms near extraordinary vertices*, Computer Aided Geometric Design, 12 (1995), pp. 153–174.

[13] J. Schweitzer, *Analysis and Application of Subdivision Surfaces*, PhD thesis, Department of Computer Science and Engineering, University of Washington, Seattle, Washington 98195, Aug. 1996. Technical Report UW-CSE-96-08-02.